



## Backwash process of marine macroplastics from a beach by nearshore currents around a submerged breakwater



Tomoya Kataoka<sup>a</sup>, Hirofumi Hinata<sup>b,\*</sup>, Shigeru Kato<sup>c</sup>

<sup>a</sup> Coastal Zone Systems Division, Coastal, Marine and Disaster Prevention Department, National Institute for Land and Infrastructure Management, 3-1-1 Nagase, Yokosuka, Kanagawa 239-0826, Japan

<sup>b</sup> Department of Civil and Environmental Engineering, Faculty of Engineering, Ehime University, 3 Bunkyo-cho, Matsuyama, Ehime 790-8577, Japan

<sup>c</sup> Department of Architecture and Civil Engineering, Toyohashi University of Technology, 1-1 Hibarigaoka, Tempaku, Toyohashi, Aichi 441-8580, Japan

### ARTICLE INFO

#### Article history:

Received 31 August 2015

Received in revised form 22 October 2015

Accepted 23 October 2015

Available online 11 November 2015

#### Keywords:

Marine macroplastics

Residence time

Submerged breakwater

Nearshore current

Mark-recapture experiment

### ABSTRACT

A key factor for determining the residence time of macroplastics on a beach is the process by which the plastics are backwashed offshore (backwash process). Here, we deduced the backwash process of plastic fishing floats on Wadahama Beach based on the analysis of two-year mark-recapture experiments as well as nearshore current structures revealed by sequential images taken by a webcam installed at the edge of a cliff behind the beach. The analysis results revealed the occurrence of a combination of offshore currents and convergence of alongshore currents in the surf zone in storm events around a submerged breakwater off the northern part of the beach, where 48% of the backwashed floats were last found. We conclude that the majority of the floats on the beach were transported alongshore and tended to concentrate in the convergence zone, from where they were backwashed offshore by the nearshore currents generated in the events.

© 2015 Elsevier Ltd. All rights reserved.

### 1. Introduction

It is well known that the most likely sources for generating small plastic fragments in the ocean are beaches because plastic debris lying on a beach quickly undergoes photo-oxidative degradation through exposure to solar ultraviolet radiation and the heat of the sand (Andrady, 2011). Also, lead stearate ( $\text{Pb}(\text{C}_{18}\text{H}_{35}\text{O}_2)_2$ ) used as an additive for plastic production could leach from the surface of a stranded PVC (polyvinyl chloride) fishing float into the beach with the aid of rainfall (Nakashima et al., 2012). Kataoka and Hinata (2015) recently demonstrated that estimating the residence time of macroplastics (>20 mm diameter; see Barnes et al., 2009) on a beach allows us to evaluate the amount of small plastic fragments generated on the beach and that of lead stearate leaching into the beach from the macroplastics, by applying a linear system analysis.

Conducting 20-month mark-recapture (MR) experiments using plastic floats on Wadahama Beach, Nii-jima Island and considering the beach as a linear black box describing the input–output behavior of the floats, we successfully estimated the average residence time of the floats on the beach as well as the overall responses of the beach to idealized float inputs (Kataoka et al., 2013). The floats stranded on the beach were eventually backwashed offshore into the coastal sea

resulting in a residence time of 209 days. By understanding how the floats disappear from the beach (hereinafter, “backwash process”), we can grasp which factors determine the floats’ residence time on the beach. This comprehensive understanding will allow us to estimate the residence time of the floats on other beaches without conducting long-term, labor-intensive MR experiments. In our previous study, the backwash process of the floats was not fully analyzed except for the estimation of the diffusion coefficient, which determines the offshore flux of the floats from the entire beach to the coastal sea.

Several studies have investigated the accumulation of marine debris on multiple beaches (e.g., Garrity and Levings, 1993; Bowman et al., 1998; Williams and Tudor, 2001; Barnes et al., 2009; Ryan et al., 2014; Smith et al., 2014). However, the behavior of plastic debris and its temporal variability on a beach are not well understood. In the present study, we attempted to clarify the backwash process of the plastic floats from Wadahama Beach by analyzing the long-term MR experiment data, wind and wave statistics and nearshore current structures using images taken by a webcam system installed at the edge of a cliff behind the beach.

The purpose of this study is, in other words, to understand the behavior of backwashed floats in high wave events. However, tracking data on the backwashed floats when they were transported offshore from the beach could not be directly obtained from our MR experiments. Therefore, we deduced the backwash process based on the alongshore movements of the remnant floats. First, we investigated the behavior of the floats on the beach based on the MR experiments,

\* Corresponding author at: Department of Civil and Environmental Engineering, Faculty of Engineering, Ehime University, 3 Bunkyo-cho, Matsuyama, Ehime 790-8577, Japan.  
E-mail address: [hinata@cee.ehime-u.ac.jp](mailto:hinata@cee.ehime-u.ac.jp) (H. Hinata).

in which the positions of the floats were recorded until their disappearance from the beach. Then we compared the behavior with the near-shore current structures visualized by the contrast in color between turbid beach waters generated in high wave events and clean offshore waters, and deduced the backwash process of the plastic floats from the beach.

## 2. Materials and methods

### 2.1. Study site

Wadahama Beach is located on the west coast of Nii-jima Island, Japan (Fig. 1(a)). The beach is approximately 900 m long and 30–50 m wide with coarse sand having a mean sediment diameter of  $d_{50} = 1.43$  mm; a promontory and concrete blocks form the northern and southern boundaries, respectively (Fig. 1(b), (c)). The beach is classified as intermediate with a beach slope ( $\tan \beta$ ) ranging from 0.09 ( $\beta = 5^\circ$ ) to 0.18 ( $\beta = 10^\circ$ ) (Wright and Short, 1984). An escarpment with an average angle of about  $35^\circ$  connects the beach to the coastal hinterland (Fig. 1(b)). This steep escarpment blocks the migration of marine debris onto the hinterland except for lower-density debris such as plastic PET bottles, plastic sheets and plastic bags.

From the analysis of tide levels recorded at the JMA tidal station on Oshima Island, which is situated about 50 km north of Nii-jima Island

(black circle in Fig. 1(a)), the high water level (HWL), mean water level (MWL) and low water level (LWL) are, respectively, 67.9 cm, 18.8 cm and  $-84.2$  cm relative to Tokyo Peil (mean sea level at Tokyo Bay) (Fig. 1(b)). Approximately 100 m from the shoreline, at a depth of 6 m, there are four submerged breakwaters (SBs) of 150 m (SB1), 100 m (SB2), 250 m (SB3) and 250 m (SB4) in length (Fig. 1(b)). The crest of the SBs is 35 m wide and 1.5 m below the MWL. SBs play an important role in determining nearshore current structure by breaking waves above the SB (e.g., Ranasinghe and Turner, 2006).

### 2.2. Target items

The target items for the MR experiments are three types of plastic fishing floats (Fig. 1(d)) as in our previous study (Kataoka et al., 2013). Dimensions and average weight of the floats measured in situ are as follows: Type 1:  $13.0$  cm  $\times$   $\phi_{max}$  2.4 cm, 38.8 g; Type 2:  $13.1$  cm  $\times$   $\phi_{max}$  7.8 cm, 116.9 g; and Type 3:  $11.0$  cm  $\times$   $\phi_{max}$  1.9 cm, 12.8 g. All three types of floats are distributed on beaches from the northernmost to southernmost ends of the Japanese Archipelago. Thus, in the future, the backwash process of these floats on Wadahama Beach can be compared with that on other beaches.

In the present study, we assumed that the behavior of the floats on Wadahama Beach was hardly affected by winds. In actuality, we observed almost no wind-induced motion of the floats on the beach

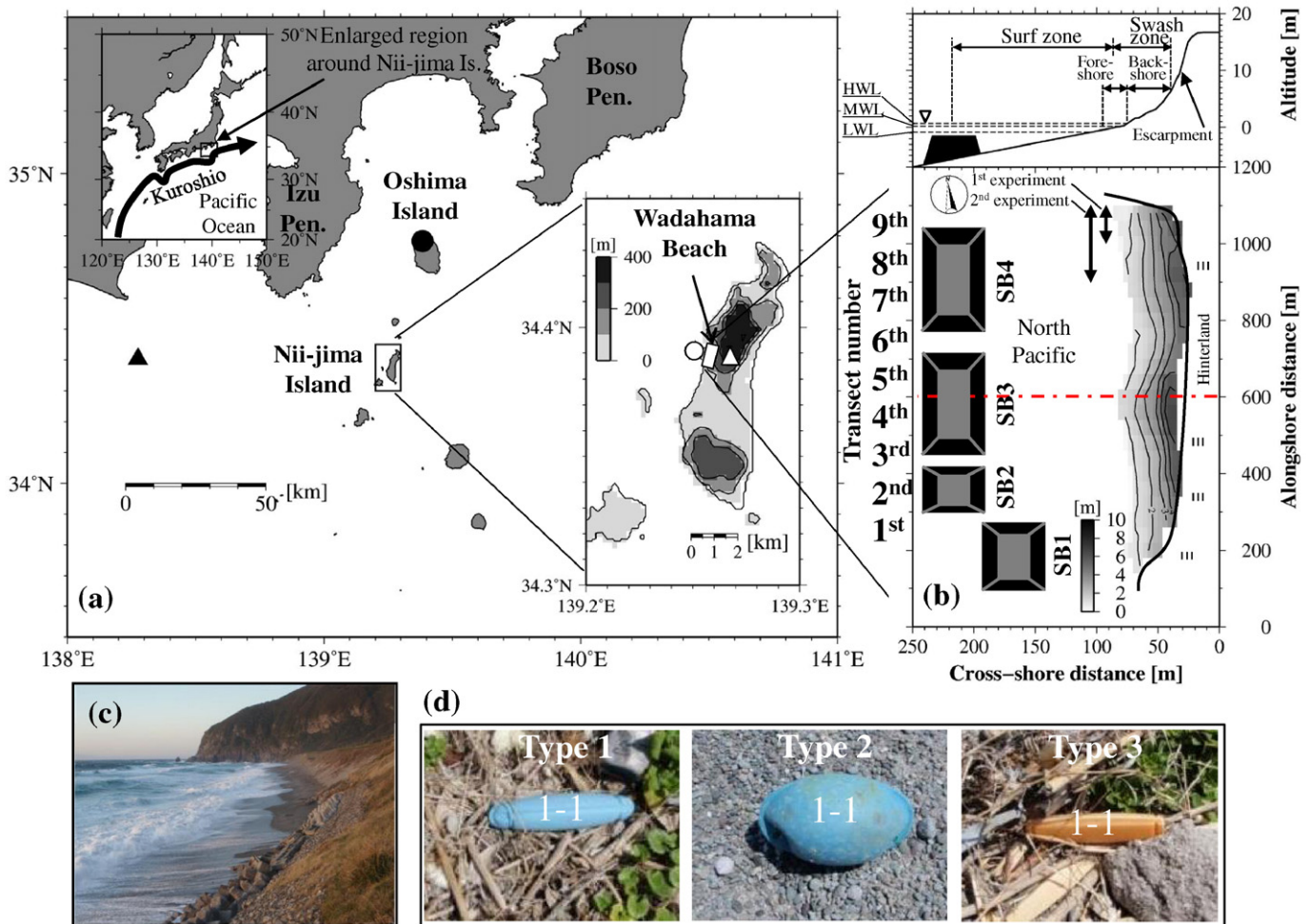


**Fig. 1.** (a) Location of Nii-jima Island, wave observation (black triangles) and tide observation sites (black circles). On the enlarged map of Nii-jima Island, contour lines and gray-white gradation denote the altitudes of Nii-jima Island. White circles and triangles indicate the location of surface wind observation and webcam sites, respectively. (b) Enlarged map of Wadahama Beach showing the altitudes relative to Tokyo Peil (contour lines and gray-white gradation). Note that the scale in the latitudinal direction is 3.2 times as large as that in the longitudinal direction. The upper panel of (b) shows the cross-sectional beach topography along the red dash-dotted line in the lower panel. The black boxes in panel (b) denote submerged breakwaters (SBs). (c) View of Wadahama Beach from the south in a storm event. (d) Photos of target items.

even in the beach surveys during the strong northwesterly winter monsoon conditions. Also, no floats were found on the coastal hinterland over the steep escarpment. Thus, we consider that the floats disappeared from the beach by being backwashed offshore due to nearshore currents (Fig. 1(c)).

### 2.3. Mark-recapture (MR) experiments and beach topographic measurements

The MR experiments were conducted since September 2011 at one- to three-month intervals (Table 1). The average interval was 53 days. The first and second experiments were carried out in the northernmost 100- and 200-m-long areas, respectively (Fig. 1(b)), while the other experiments covered the whole beach. All three types of floats on the beach were collected, numbered with a permanent marker and replaced where they were found. The marked number consisted of the experiment number and a sequential number allocated to each type of float (Fig. 1(d)). A thorough search for the floats was conducted until no unnumbered target items could be found by repeated observations. The position of each item was recorded by a handheld global positioning system (GPS) receiver (GPSMAP® 60CSx, Garmin Ltd.) with a measurement error of about  $\pm 3$  m.

For all analyses in the present study, we divided the beach into nine transects measuring 100 m long in the alongshore direction as shown on the left side of Fig. 1(b). In addition, the floats were classified into three states: newly washed ashore (immigrant), backwashed offshore (emigrant), or remaining on the beach surface (remnant) for the interval between the previous and present MR experiments (hereinafter, “experiment period”). In Table 1, the number of remnants includes re-emerged floats that were not recovered in the previous surveys but were found in the present survey. However, the ratio of re-emerged floats to remnants is small (10% on average). The abundance of re-emergence is added to the cohort population of the previous experiments.

The beach elevation was measured by using a real-time kinematic GPS system (Trimble® 5800 II, Trimble Navigation Ltd.) with a horizontal and vertical measurement error of about  $\pm 5$  mm. The alongshore and cross-shore distance between adjacent measurement points was about 10 m and about 5 m, respectively. The raw measured data was interpolated to a grid point with both alongshore and cross-shore spacing of 5 m using a nearest-neighbor algorithm with a spline function (McKinley and Levine, 1998).

### 2.4. Observation of sea surface wind, waves and nearshore current structure

We analyzed the sea surface wind and wave data respectively observed by the Advanced Scatterometer (ASCAT) and by the GPS buoy (e.g., Kato et al., 2011) established at about 90 km west of Nii-jima Island (black triangle in Fig. 1(a)) by the Nationwide Ocean Wave Information Network for Ports and Harbours (NOWPHAS). The sea surface wind data has been gridded using an optimal interpolation method developed by Kako et al. (2011). We used the sea surface wind data at a grid point located in front of Wadahama Beach (white circle in Fig. 1(a)). The wave runup height on Wadahama Beach was estimated using the wave statistics calculated from the data obtained by the GPS buoy. Details of the estimation of the runup height are described in the Appendix A.

The webcam system developed by Kataoka et al. (2012) has been installed at the edge of the cliff behind the beach since December 2014 (white triangle in Fig. 1(a)). The webcam is programmed to operate for 15 min every 1 h from 7:00 to 17:00 (Japan standard time), thus providing eleven 15-min videos every day. The videos are recorded on an SDHC card installed in the webcam. From our analysis of the videos, we understood the qualitative features of nearshore currents visualized by the contrast in color between turbid beach waters and clear offshore waters and its temporal evolution.

## 3. Results

### 3.1. Wave runup height on Wadahama Beach

Fig. 2 shows the temporal variability of sea surface wind (Fig. 2(a)) and wave runup height (Fig. 2(c)). In October to March (S1), southwesterly winds and waves prevailed when the runup height was greater than 2 m (Fig. 2(b) and (d)). Northwesterly winds intensified by the East Asian Monsoon rarely developed longer-period wind waves under the small fetch length from Honshu Island to the GPS buoy station (see Fig. 1(a)). In April to September (S2), the sea surface wind was generally weaker compared with that in S1, while the estimated runup height was intermittently much greater than that in S1 because of the incidence of longer-period waves (see Appendix A) mainly from the south-southwest (Fig. 2(d)). These generally originated from low-pressure systems (e.g., typhoons) in the southern region of Nii-jima Island.

For the actual incident waves to Wadahama Beach as well, the smaller fetch length between Honshu Island and Nii-jima Island (see Fig. 1(a)) basically limits the evolution of northerly wind waves. Thus, the wave statistics and the estimated runup height based on the wave statistics at the GPS station are considered useful for identifying storm events on Wadahama Beach.

### 3.2. Re-estimation of float residence time on the whole Wadahama Beach

The total number of remnant floats (hereinafter, “cohort population”) newly found at each MR experiment from September 30, 2011 to August 31, 2013 is shown in Table 1. The cohort population decreases exponentially. We approximated the cohort population normalized by the initial population as the exponential function ( $h(t) = \exp(-ft)$ ) with a 95% confidence level ( $n = 104$ ,  $R^2 = 0.852$ ,  $P = 6.47 \times 10^{-47} < 0.05$ ) as follows:

$$h(t) = \begin{cases} \exp(-4.471 \times 10^{-3}t), & t \geq 0, \\ 0, & t < 0, \end{cases} \quad (1)$$

where  $t$  is elapsed time in days from the MR experiment day. From the integral of this function from  $t = 0$  to infinity, the average residence time of the floats on the whole beach is  $\tau_r = 1/f = 224$  days, that is, about 7.5 months. The margin of error of the coefficient  $f$  was estimated as  $0.340 \times 10^{-3} \text{ (day}^{-1}\text{)}$  by a  $t$ -distribution with a 95% confidence limit. Thus, the residence time has a 95% confidence interval from 208 days ( $= 1 / (4.471 \times 10^{-3} + 0.340 \times 10^{-3})$ ) to 242 days ( $= 1 / (4.471 \times 10^{-3} - 0.340 \times 10^{-3})$ ). The exponential decay of the cohort population means that the cohort population decreased at a constant rate of  $0.5\% \text{ day}^{-1}$  determined as  $1 - \exp(-1/224) = 0.005$ .

Kataoka et al. (2013) previously estimated the average residence time on Wadahama Beach based on the 20-month exponential decay from September 30, 2011 to May 8, 2013, which was 209 days with the 95% confidence interval from 192 to 230 days ( $n = 77$ ,  $R^2 = 0.852$ ,  $P = 4.97 \times 10^{-35} < 0.05$ ). The average residence time increased slightly by adding the cohort population measured on June 27 and August 31, 2013. To estimate the “true” average residence time on Wadahama Beach, it might be necessary to continuously conduct the MR experiment. Nevertheless, the previously reported residence time (209 days) is within the range of the 95% confidence interval of the re-estimated residence time in this study (i.e.,  $208 \text{ days} < \tau_r < 242 \text{ days}$ ). Hence, here we considered the average residence time of the floats on Wadahama Beach as 224 days.

### 3.3. Spatial distribution and alongshore movement of the floats on the beach

Fig. 3 shows the beach topography and the positions of the immigrant, remnant and emigrant floats measured at each MR experiment

**Table 1**

Number of floats recovered by the MR experiments and cohort population and abundance of re-emergence (within parentheses) in each MR experiment.

Experiment no.	1		2		3		4		5		6		7	
Experiment date	2011/09/30		2011/10/27		2011/11/24		2011/11/26		2012/01/26		2012/03/23		2012/06/29	
Number of days		27		28		2		61		57		98		53
Number of storm events		1		2		1		3		3		16		4
Classification of season		1		1		1		1		1		2		2
Immigrant	47		77		61		20		18		18		136	
Remnant	0 (0)		36 (0)		105 (1)		163 (4)		139 (7)		112 (12)		85 (22)	
Total population	47		113		166		183		157		130		221	
Emigrant	0		11		8		3		44		45		45	
<i>Cohort population<sup>d</sup></i>														
No. 1	47 (0)		36 (0) <sup>b</sup>		34 (1)		34 (2)		28 (2)		17 (0)		12 (3)	
No. 2	-		77 (0)		71 (0)		71 (2)		52 (5)		38 (2)		27 (8)	
No. 3	-		-		61 (0)		58 (0)		44 (0)		34 (6)		25 (7)	
No. 4	-		-		-		20 (0)		15 (0)		12 (4)		6 (1)	
No. 5	-		-		-		-		18 (0)		11 (0)		8 (3)	
No. 6	-		-		-		-		-		18 (0)		7 (0)	
No. 7	-		-		-		-		-		-		136 (0)	
No. 8	-		-		-		-		-		-		-	
No. 9	-		-		-		-		-		-		-	
No. 10	-		-		-		-		-		-		-	
No. 11	-		-		-		-		-		-		-	
No. 12	-		-		-		-		-		-		-	
No. 13	-		-		-		-		-		-		-	
No. 14	-		-		-		-		-		-		-	

<sup>a</sup> The abundance of reemergence is added to the cohort population of the previous experiments.<sup>b</sup> Cohort population of no. 1 in the second experiment is not used in the calculation of the residence time because the second experiment was carried out in the northernmost 200 m-long area.

Table 1 (continued)

Experiment no.	8	9	10	'11	12	13	14
Experiment date	2012/08/21	2012/11/08	2012/12/27	2013/02/27	2013/05/08	2013/06/27	2013/08/31
Number of days		79	49	62	70	50	65
Number of storm events		20	3	3	3	1	4
Classification of season		2	1	1	2	2	2
Immigrant	26	57	20	28	191	64	21
Remnant	188 (1)	97 (13)	141 (12)	137 (5)	123 (60)	294 (6)	305 (14)
Total population	214	154	161	165	314	358	326
Emigrant	33	117	13	24	42	20	53
<i>Cohort population<sup>a</sup></i>							
No. 1	10 (0)	6 (3)	6 (0)	6 (1)	6 (3)	5 (0)	5 (0)
No. 2	23 (1)	12 (4)	10 (2)	8 (0)	7 (2)	7 (0)	4 (1)
No. 3	21 (0)	13 (2)	11 (2)	10 (0)	7 (4)	7 (0)	6 (2)
No. 4	5 (0)	4 (1)	4 (3)	4 (0)	1 (0)	1 (1)	1 (0)
No. 5	7 (0)	4 (0)	4 (2)	2 (0)	2 (1)	2 (0)	2 (0)
No. 6	6 (0)	2 (0)	2 (1)	2 (0)	1 (0)	1 (1)	1 (0)
No. 7	116 (0)	48 (3)	46 (2)	38 (1)	35 (22)	34 (1)	27 (2)
No. 8	26 (0)	8 (0)	8 (0)	7 (0)	6 (3)	5 (1)	4 (0)
No. 9	–	57 (0)	50 (0)	44 (3)	31 (18)	29 (2)	29 (0)
No. 10	–	–	20 (0)	16 (0)	14 (7)	11 (0)	11 (1)
No. 11	–	–	–	28 (0)	13 (0)	13 (0)	12 (1)
No. 12	–	–	–	–	191 (0)	179 (0)	158 (7)
No. 13	–	–	–	–	–	64 (0)	45 (0)
No. 14	–	–	–	–	–	–	21 (0)

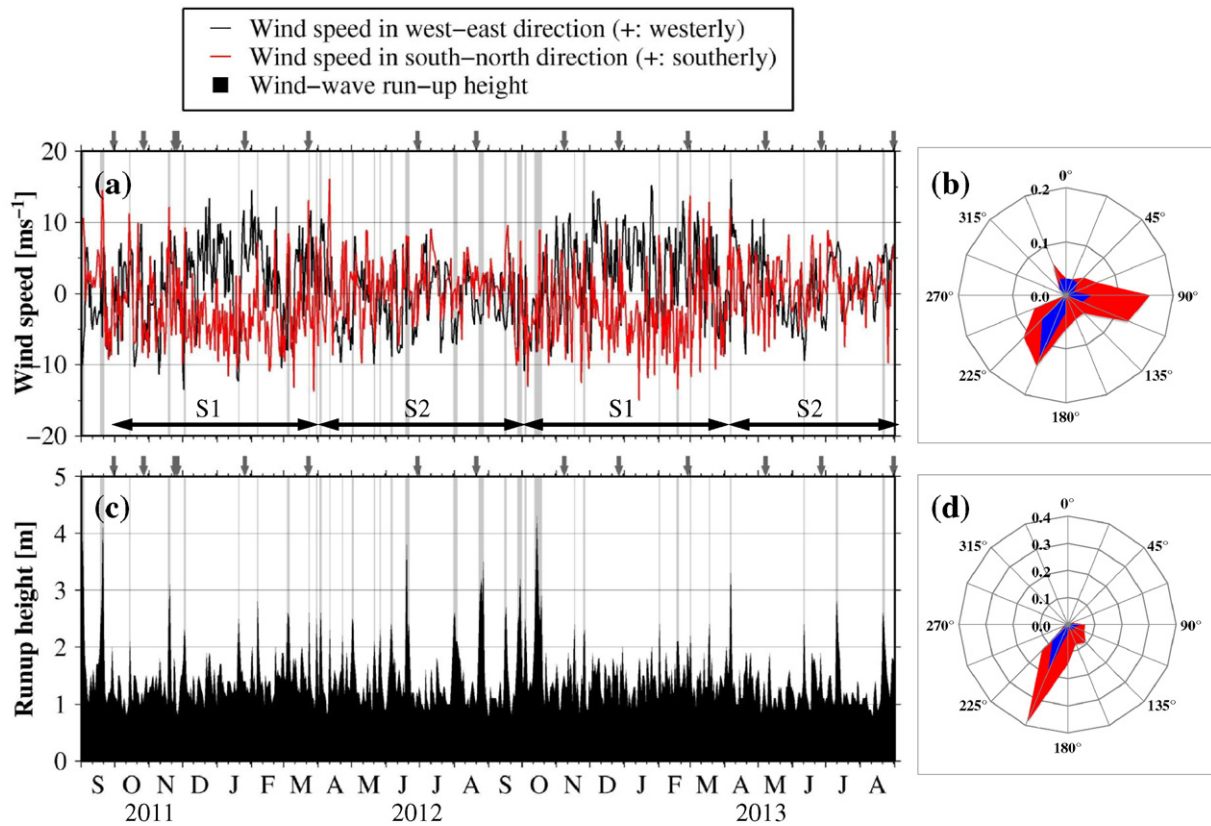


**Fig. 2.** Time series of (a) wind component speeds observed by ASCAT and (c) wave runup height estimated based on the daily wave statistics observed at about 90 km west of Nii-jima Island (black triangle in Fig. 1(a)). The meanings of lines and their colors are shown in the top box. Light-gray bars in panels (a) and (c) indicate the duration of storm events, which is when the runup height was higher than 2 m. Gray arrow indicates the MR experiment date as described in Table 1. Rose diagrams of wind and wave directions in storm events are shown in panels (b) and (d), respectively. The wind and wave directions are expressed in degrees clockwise from the north; for instance, a wave and wind coming from the south are given as 180°. Blue (red) plane indicates the frequencies of wind and wave direction in S1 (S2).

from November 24, 2011 to August 31, 2013. Note that the positions of the floats recorded in the experiments on September 30 and October 31, 2011 are not shown because these two experiments were conducted only in the northernmost area (see Section 2.3). The positions of emigrant floats denote the positions of those found at the previous MR experiment. The shoreline of the beach consistently advanced seaward (i.e., salient) in the central area ranging from 500 to 700 m and in the northern area ranging from 900 to 1100 m, suggesting the generation of a consistent nearshore current structure in the surf zone off the beach, which was probably controlled by the SBs.

The floats were consistently distributed at a beach elevation higher than 2 m (Fig. 3). This indicates that the floats were moved by swash waves reaching a beach elevation higher than 2 m, and conversely, were hardly moved by tidal fluctuations because the floats were washed up at much higher elevations than the HWL (bold broken line in Fig. 3). In the present study, we define the duration when the runup height was higher than 2 m as a storm event (light-gray bars in Fig. 2(a) and (c)). The total number of events that occurred in S2 (48 times) is three times greater than that in S1 (16 times) because of the longer-period wave incidence to the beach in S2 (Table 1).

We summed up the number of immigrant, remnant and emigrant floats in each 100-m-long transect obtained at every MR experiment and calculated the immigrant ( $I_n$ ), remnant ( $R_n$ ) and emigrant ( $E_n$ ) ratios by dividing the three totals for each transect by the corresponding totals for the whole beach. Note that we calculated  $I_n$  ( $R_n$  and  $E_n$ ) by using the data from the third (fourth) to fourteenth (fourteenth) MR experiments. Here,  $n$  denotes the transect number ( $n = 1, 2, \dots, 9$ ). The immigrant, remnant and emigrant ratios and their spatial distribution are shown in Table 2 and Fig. 4(a), respectively. Looking at the seventh

transect, for instance, 29% (24%) of all remnant (immigrant) floats were (newly) found in this transect at the present MR experiment; 25% of all floats backwashed offshore during the previous and present experiments were last found in this transect.

Overall, the distribution patterns of the three ratios were similar in reference to the local maxima of the fourth and seventh transects. Nevertheless, the sum of the remnant and emigrant ratios in the northern area from 800 to 1100 m of alongshore distance (65% and 70%, respectively) was even higher than that of the immigrant ratio (52%) in the same area (Table 2). The difference suggests that the floats were likely to concentrate in the northern area in the backwash process, since the remnant and emigrant floats had stayed on the beach for a longer time and had more chances to be transported by waves and coastal currents in the storm events than the immigrant floats, and thus the difference reflects the movement of the floats during the storm events.

Fig. 5 shows the temporal change of the alongshore position of the remnant floats of each cohort, that is, the alongshore movement of the floats. It is noted that the floats did not move directly in the alongshore direction on the beach as mentioned in Section 2.2. When the floats that backwashed to the sea returned onto the beach, their new positions were different from their original ones before backwashing. The remnant floats tended to converge mainly in the seventh transect with the cohort population decreasing in the backwash process. This resulted in the difference in the distribution between the ratios in the northern area as mentioned above. Dividing the alongshore transport distance of the remnant floats by the total duration of the storm events in each experiment period, we calculated the temporal mean alongshore movement velocities of the remnant floats in the events (hereinafter, “transport velocity”) and found that the transport velocity was in



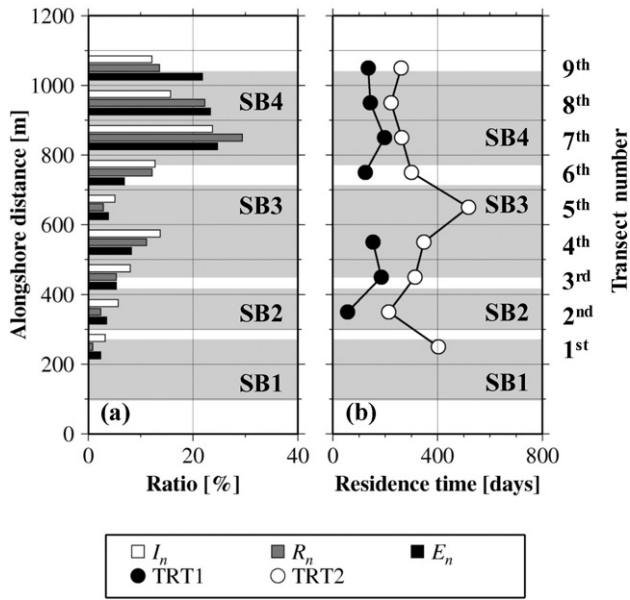


Fig. 4. Alongshore distributions of immigrant ratio ( $I_n$ ), remnant ratio ( $R_n$ ), emigrant ratio ( $E_n$ ) (a) and transect residence times (TRTs) (b). The meanings of symbols and their colors are shown in the bottom box. Light-gray area indicates the alongshore position of the SB. The transect numbers are shown on the right side of panel (b).

having a shorter TRT2 and a smaller difference between TRT1 and TRT2 are possible transects where the floats were backwashed offshore, because the combination of a shorter TRT2 and smaller difference means that the floats tend to be backwashed offshore rather than be moved to other transects.

In the same way as the estimation of the average residence time on the whole beach (see Section 3.1), the average TRTs can be estimated by approximating the decrease in the population of remnant floats originating in each transect as an exponential function:

$$h_n(t) = \frac{P_n(t_k + t)}{P_n(t_k)} = \begin{cases} \exp(f_n t), & t \geq 0, \\ 0, & t < 0, \end{cases} \quad (2)$$

where  $P_n(t_k)$  is the number of immigrant floats stranded in the  $n$ -th transect at the  $k$ -th MR experiment conducted at  $t_k$  (transect cohort population).  $P_n(t_k + t)$  is the transect cohort population at  $t_k + t$  in the  $n$ -th transect (on the whole beach) for calculating TRT1 (TRT2).  $t$  is the elapsed time in days from  $t_k$ . From the population decay of the transect cohorts with respect to  $t$ , we defined the exponential function. TRTs of the  $n$ -th transect are defined as  $1/f_n$ .

TRT1 and TRT2 are shown in Table 2 and Fig. 4(b). TRT1 of the first and fifth transects having a much smaller cohort population could not be calculated because the population decay was not significantly approximated as an exponential function. Overall, TRT1 was shorter than the average residence time of all floats on the whole beach (i.e., 224 days), because the transect cohort population decreased by moving to other transects as well as being backwashed offshore. On the other hand, TRT2 ranged widely from 213 to 518 days and was longer at the center of the beach and became shorter in the northern and southern

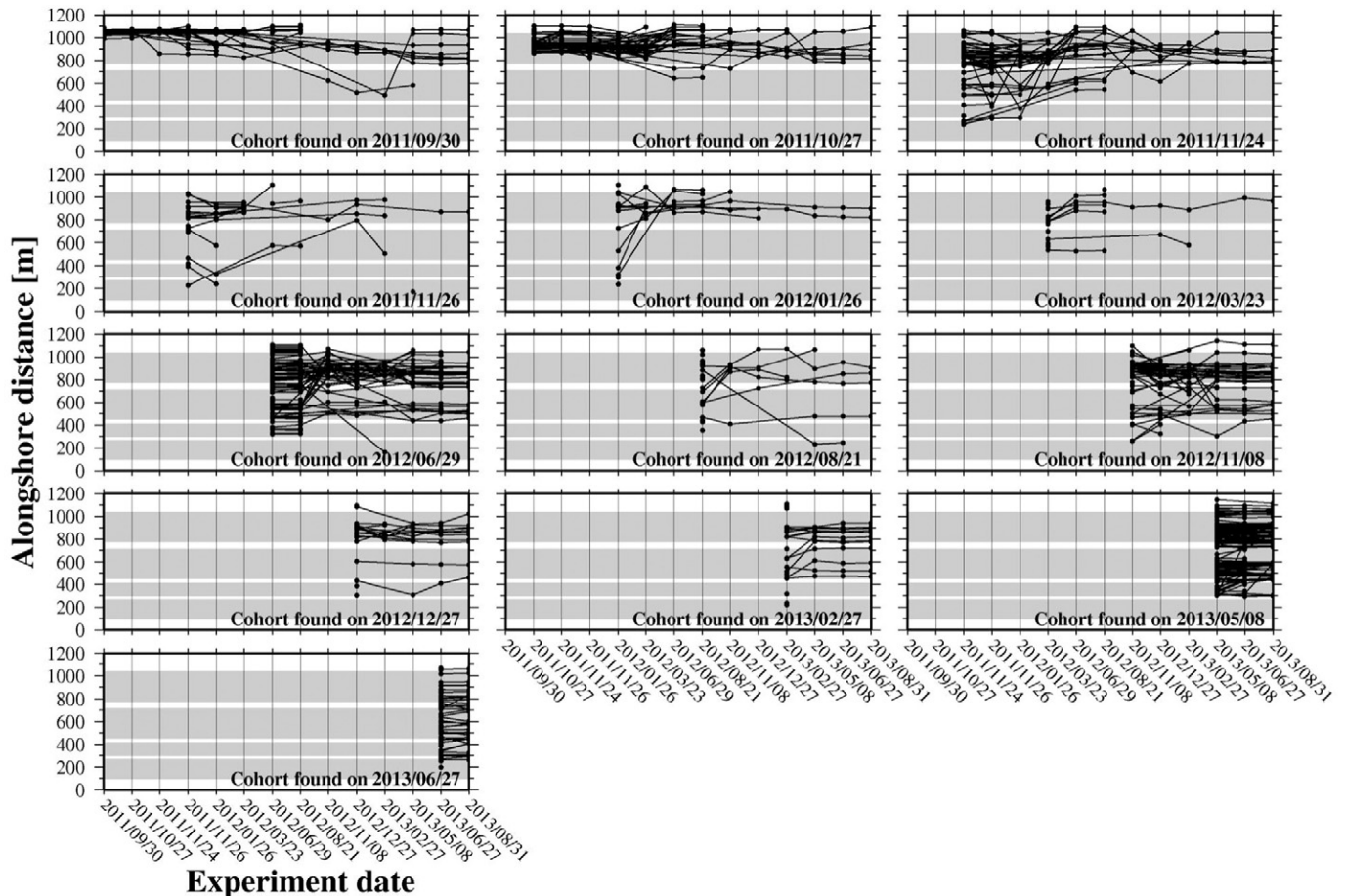


Fig. 5. Alongshore movements of the floats on the beach from when they were newly found to August 31, 2013. Light-gray area indicates the alongshore position of the SB.

transects. TRT2s of the second and eighth transects were shorter than 224 days. The difference in TRTs of the seventh and eighth transects, where 48% of the total emigrant floats were last found (Table 2), was significantly smaller than that of the other transects. These results suggest that the seventh and eighth transects were the most likely backwash transects. In other words, in terms of nearshore hydrodynamics, offshore currents would occur in the surf zone near these transects in the storm events. In addition, the alongshore float movements (Fig. 5) indicate that alongshore current convergence mainly occurred off the seventh transect.

### 3.5. Nearshore current structures around SB4

Fig. 6(a) and (b) shows snapshots of the nearshore current structures off the fifth to ninth transects in storm events, as recorded by the webcam at 12:19 on December 21, 2014 (corresponding to S1) and at 14:11 on July 26, 2015 (corresponding to S2), respectively. Also, 15-min animations made from the images taken every 5 s can be viewed online in the electronic version of this article (Appendix B).

From the wave and surface wind records, the mean surface wind and wave directions were respectively  $311^\circ$  and  $238^\circ$  measured clockwise from the north on December 21, 2014. The estimated runup height was 3.2 m. Regarding the wave directions observed in storm events in S1 during the MR experiment period, the waves propagated from the southwest, while the northwesterly wind prevailed on this day. However, based on the images, the waves propagated nearly normal to the beach probably due to wave refraction and diffraction. The incident waves were broken above SB4 resulting in the onshore mass transport and the turbid beach waters flowed offshore mainly from the seventh and eighth transects through the gap between SB4 and SB3 and along the promontory. This combination of onshore–offshore currents around SB4 is expected to induce northward and southward alongshore currents in the lee of SB4 (broken arrows in Fig. 6(a)), resulting in the generation of horizontal convergence off the seventh transect. Off SB4, the turbid beach waters originating in the surf zone were advected southward due to offshore current, which was presumably driven by wind. However, we cannot exclude the possibility of tidal currents and/or the Kuroshio filaments. It is interesting to note that offshore clear waters intruded into the surf zone through the gaps between SB4 and the promontory and between SB3 and SB4.

On July 26, 2015, the estimated runup height was 4.1 m and the mean wind and wave directions were respectively  $263^\circ$  and  $215^\circ$  as observed in storm events in S2 during the MR experiment period. The nearshore current structure was similar to that generated on December 21, 2014 except that no offshore water intrusion occurred in the gap between SB4 and the promontory. Off SB4, northward current was dominant on that day.

Overall current structure in the surf zone on the two days corresponds well with that generated behind a submerged breakwater

under normal wave incidence conditions described in previous studies (e.g., Ranasinghe and Turner, 2006). This suggests that the wave-driven currents dominated over the currents driven by other forces in the surf zone, whereas the currents driven by other forces were dominant off SB4 in the storm events.

## 4. Discussion and conclusions

The images and animations of the nearshore current structure off the northern part of the beach (Fig. 6) confirmed the occurrence of the combination of offshore currents in the lee of SB4 and alongshore current convergence mainly off the seventh transect deduced from the MR experiment results (Figs. 4, 5). The current structure corresponds well with that generated around a SB as described in previous studies (e.g., Ranasinghe and Turner, 2006). The confirmation allows us to conclude that the majority of remnant floats on the beach were transported alongshore and tended to concentrate in the convergence zone and were backwashed offshore by the wave-driven nearshore currents. The backwash process speculated in our previous study (Fig. 7 in Kataoka et al., 2013) has been improved as illustrated in Fig. 7 except for the process in the central–southern area of the beach because of the limited coverage of the webcam. Although a southwesterly wind generally prevails in a storm event, current off SB4 transports the turbid water from the surf zone southward when a northwesterly wind prevails as on December 21, 2014. The backwash process in the central–southern part of the beach is also expected to be determined by the nearshore current structure, which is probably controlled by the distribution of SBs. The consistent shoreline with the salient in the central and northern areas suggests the generation of a consistent nearshore current structure in the surf zone off the beach. The large remnant ratio in the northern corner (Fig. 4a) would result from the overall northward transfer of the floats on the beach under the northward winds and waves prevailing during the storm events (Fig. 2b and d).

The transport velocities of the remnant floats were much smaller than those of the nearshore currents (see Section 3.3). The transport velocities were evaluated based on the remnant float movements, but not by the emigrant float movements, which might be of the same order of magnitude as the nearshore current velocities. From all the remnant float movements during November 24, 2011 and August 31, 2013, it was found that 89% of the recaptured floats were transported within a distance of less than 100 m, while 11% of the floats were greatly transported over a longer distance than 100 m during one experiment period. This suggests that the majority of the remnant floats are transported into the surf zone and washed ashore onto the same transect by swash waves repeatedly and intermittently in the storm events. In this process, on average, they would be gradually transported in the alongshore direction by the alongshore wind- and wave-driven



**Fig. 6.** Snapshot of nearshore currents taken by the webcam at 12:19 on December 21, 2014 (a) and at 14:11 on July 26, 2015 (b) visualized by the contrast in color of turbid beach waters and clear offshore waters and its temporal evolution (solid arrows). Broken arrows are deduced currents. 15-min animations made from the images taken every 5 s are also available online in the electronic version of this article (Appendix B).

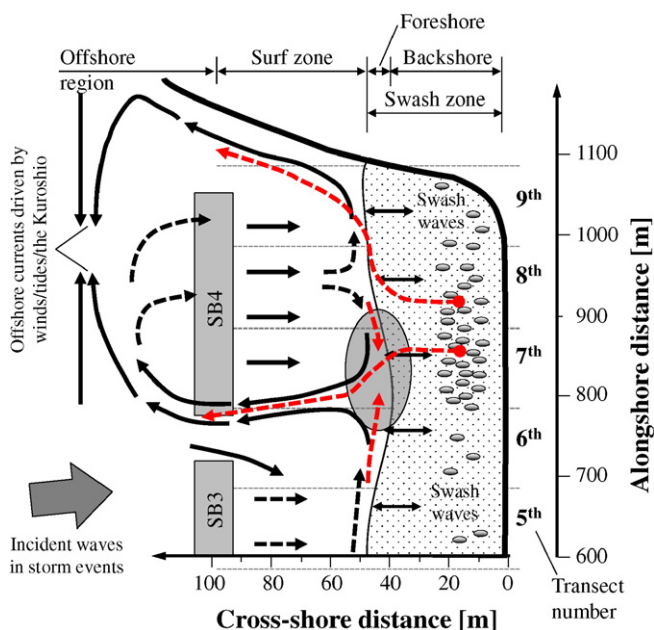


Fig. 7. Schematic image of nearshore current structure and associated backwash process of the floats from Wadahama Beach. Black (red) broken arrow indicates deduced nearshore current (backwash process). Horizontal convergence of alongshore current mainly occurs in the shaded area.

currents. In addition, we assumed that the remnant floats had been moving during the storm events and calculated the transport velocity by dividing the alongshore transport distance of the remnant floats by the duration of the storm events (see Section 3.3), whereas in actuality they would be intermittently moved in the alongshore direction by the combination of swash waves and alongshore currents. Therefore, although the transport velocities were much smaller than the nearshore current velocities, we believe that the movements of the remnant floats reflect the alongshore current structure.

The final goal of this study is to establish a mathematical model to estimate the average residence time of marine plastics on the beach. Considering that the backwash process was controlled by the nearshore currents in the storm events, the average residence time on the beach is expected to be determined by the frequency of the storm event occurrence and nearshore current structures, that is, the scales of the horizontal length and velocity of the currents. We can understand the frequency and qualitative features of the nearshore currents based on the webcam images, as demonstrated in this study. In the near future, we will measure the scales of the nearshore current structures using the tracking data of small buoys equipped with the GPS receiver distributed in the surf zone in the storm events. An understanding of the scales and the frequency will enable us to estimate the diffusion coefficient of the plastic floats, which determines the offshore flux of the floats from the beach and thus the residence time of the floats on the whole beach.

#### Acknowledgments

This research was supported by the Environment Research and Technology Development Fund (B-1007 and 4-1502) of the Ministry of the Environment, Japan and by JSPS KAKENHI Grant Numbers 23656309, 25820234 and 26630231.

#### Appendix A. Estimation of wave runup height on Wadahama Beach

Waves are monitored by a NOWPHAS GPS buoy located about 90 km west of Nii-jima Island (black triangle in Fig. 1(a)). Data is available at [http://www.mlit.go.jp/kowan/nowphas/index\\_eng.html](http://www.mlit.go.jp/kowan/nowphas/index_eng.html). The runup

height was calculated using the daily significant wave height and period as follows

$$\frac{R}{H_0} = \xi, \quad (\text{A1})$$

where  $R$  is the runup height from MWL and  $H_0$  is the deep-water significant wave height (Hunt, 1959).  $\xi$  is the Iribarren number, which is defined as (Battjes, 1974):

$$\xi = \frac{\tan \beta}{(H_0/L_0)^{1/2}}, \quad (\text{A2})$$

where  $\tan \beta$  is the beach slope,  $L_0$  is the deep-water wave length given by  $L_0 = (g/2\pi)T_0^2$  where  $g$  is the acceleration due to gravity and  $T_0$  is the significant wave period. The beach slope was determined as  $\tan \beta = 0.14$  based on measurements of the beach topography. The Iribarren number can be interpreted as the dynamic beach steepness, comparing the beach slope to the square root of the deep-water wave steepness.

#### Appendix B. Supplementary data

Supplementary data to this article can be found online at <http://dx.doi.org/10.1016/j.marpolbul.2015.10.060>.

#### References

- Andrady, A.L., 2011. Microplastics in the marine environment. *Mar. Pollut. Bull.* 62 (8), 1596–1605.
- Barnes, D.K.A., Galgani, F., Thompson, R.C., Barlaz, M., 2009. Accumulation and fragmentation of plastic debris in global environments. *Philos. Trans. R. Soc. B* 364, 1985–1998.
- Battjes, J.A., 1974. Surf Similarity. *Proc. 14th Conf. Coastal Eng. Am. Soc. Civ. Eng.*, pp. 466–479.
- Bowman, D., Manor-Samsonov, N., Golik, A., 1998. Dynamics of litter pollution on Israeli Mediterranean beaches: a budgetary, litter flux approach. *J. Coast. Res.* 14 (2), 418–432.
- Garrity, S.D., Levings, S.C., 1993. Marine debris along the Caribbean coast of Panama. *Mar. Pollut. Bull.* 26 (6), 317–324.
- Hunt, I.A., 1959. Design of seawalls and breakwaters. *Proc. Am. Soc. Civ. Eng.* 85, 123–152.
- Kako, S., Isobe, A., Kubota, M., 2011. High-resolution ASCAT wind vector data set gridded by applying an optimum interpolation method to the global ocean. *J. Geophys. Res.* 116, D23107.
- Kataoka, T., Hinata, H., 2015. Evaluation of beach cleanup effects using linear system analysis. *Mar. Pollut. Bull.* 91 (1), 73–81.
- Kataoka, T., Hinata, H., Kako, S.I., 2012. A new technique for detecting colored macro plastic debris on beaches using webcam images and CIELUV. *Mar. Pollut. Bull.* 64 (9), 1829–1836.
- Kataoka, T., Hinata, H., Kato, S., 2013. Analysis of a beach as a time-invariant linear input/output system of marine litter. *Mar. Pollut. Bull.* 77 (1), 266–273.
- Kato, T., Terada, Y., Nishimura, H., Nagai, T., Koshimura, S., 2011. Tsunami records due to the 2010 Chile earthquake observed by GPS buoys established along the Pacific coast of Japan. *Earth Planets Space* 63, e5–e8.
- Kuriyama, Y., Nakatsukasa, T., 2000. A one-dimensional model for undertow and longshore current on a barred beach. *Coast. Eng.* 40 (1), 39–58.
- McKinley, P., Levine, M., 1998. Cubic Spline Interpolation Available at <http://online.redwoods.edu/instruct/darnold/LAPROJ/Fall98/SkyMeg/Proj.PDF>.
- Nakashima, E., Isobe, A., Kako, S.I., Itai, T., Takahashi, S., 2012. Quantification of toxic metals derived from macroplastic litter on Ookushi Beach, Japan. *Environ. Sci. Technol.* 46 (18), 10099–10105.
- Ranasinghe, R., Turner, I.L., 2006. Shoreline response to submerged structures: a review. *Coast. Eng.* 53 (1), 65–79.
- Ryan, P.G., Lamprecht, A., Swanepoel, D., Moloney, C.L., 2014. The effect of fine-scale sampling frequency on estimates of beach litter accumulation. *Mar. Pollut. Bull.* 88 (1–2), 249–254.
- Smith, S.D., Gillies, C.L., Shortland-Jones, H., 2014. Patterns of marine debris distribution on the beaches of Rottnest Island, Western Australia. *Mar. Pollut. Bull.* 88 (1–2), 188–193.
- Sonu, C.J., 1972. Field observation of nearshore circulation and meandering currents. *J. Geophys. Res.* 77 (18), 3232–3247.
- Williams, A.T., Tudor, D.T., 2001. Litter burial and exhumation: spatial and temporal distribution on a cobble pocket beach. *Mar. Pollut. Bull.* 42 (11), 1031–1039.
- Wright, L.D., Short, A.D., 1984. Morphodynamic variability of surf zones and beaches: a synthesis. *Mar. Geol.* 56 (1), 93–118.